

# 3-Aminopropyltriethoxysilane Complexation with Iron Ion Modified Anode in Marine Sediment Microbial Fuel Cells with Enhanced Electrochemical Performance

ZAI Xuerong<sup>1)</sup>, GUO Man<sup>1)</sup>, HAO Yaokang<sup>2)</sup>, HOU Shaoxin<sup>2)</sup>, YANG Zhiwei<sup>2)</sup>, LI Jia<sup>2)</sup>, LI Yang<sup>2)</sup>, JI Hongwei<sup>1)</sup>, and FU Yubin<sup>2)</sup>, \*

1) College of Chemistry and Chemical Engineering, the Key Laboratory of Marine Chemistry Theory and Technology, Ministry of Education, Ocean University of China, Qingdao 266100, China

2) School of Materials Science and Engineering, Ocean University of China, Qingdao 266100, China

(Received March 12, 2020; revised December 22, 2020; accepted December 27, 2020)

© Ocean University of China, Science Press and Springer-Verlag GmbH Germany 2021

**Abstract** Anode modification plays a key role in higher power output in marine sediment microbial fuel cells (MSMFCs). A low-molecular organosilicon compound (3-aminopropyltriethoxysilane) was grafted onto the surface of carbon felt using chemical method and a composite modified anode was prepared through organic ligands coordination  $\text{Fe}^{3+}$  for better electro-chemical performance. Results show that the biofilm resistance of the composite modified anode ( $2707\ \Omega$ ) is 1.3 times greater than that of the unmodified anode ( $2100\ \Omega$ ), and its biofilm capacitance also increases by 2.2 times, indicating that the composite modification promotes the growth and attachment of electroactive bacteria on the anode. Its specific capacitance ( $887.8\ \text{F m}^{-2}$ ) is 3.7 times higher than that of unmodified anode, generating a maximum current density of  $1.5\ \text{A m}^{-2}$ . In their Tafel curves, the composite modified anodic exchange current density ( $5.25 \times 10^{-6}\ \text{A cm}^{-2}$ ) is 5.8 times bigger than that of unmodified anode, which suggests that the electro-chemical activity of redox, anti-polarization ability and electron transfer kinetic activity are significantly enhanced. The marine sediment microbial fuel cell with the composite modified anode generates the higher power densities than the blank ( $203.8\ \text{mW m}^{-2}$  versus  $45.07\ \text{mW m}^{-2}$ ), and its current also increases by 4.4 times. The free amino groups on the anode surface expands a creative idea that the modified anode ligates the natural Fe(III) ion in sea water in the MSMFCs for its higher power output.

**Key words** 3-aminopropyltriethoxysilane; iron ion; composite modified carbon anode; electro-chemical performances; marine sediment; microbial fuel cells

## 1 Introduction

Marine instruments on ocean floor need long term power supply for themselves several years' works when human being uses them to develop ocean, but battery technology or electric cables both cannot satisfy the urgent demands till now for its short service life. Marine sediments microbial fuel cells (MSMFCs) are a new type of microbial fuel cells to harvest bioenergy from sediment for its renewable energy, long term power output, *in-situ* energy harvest on ocean floor (Ghoreishi *et al.*, 2014; Ewing *et al.*, 2017; Zhao *et al.*, 2017). The essence of electricity production is that the bacteria decompose the inorganic or organic matter in the marine sediment to generate electricity (Chen *et al.*, 2017; Zhang *et al.*, 2018; Zhou *et al.*, 2018). Though our research group has designed and utilized large scale MSMFCs to drive marine sensors (5V TD or 12V CTD) work more than 17 months

on the ocean floor in Jiaozhou Bay, its maximum power output reached 0.48 W (Zhou *et al.*, 2018), however, its lower power still limits its further application.

In the MSMFCs, anode plays a key role in harvesting more electrons from sediment bacteria. The transfer of electrons from microorganisms to anodes is one of significant factors affecting their electrochemical performance. The anodic material, its surface area and the amount of microbial enrichment can affect the anodic electron transfer and its electro-chemical performance. Among them, the anodic material acts as a carrier for microbial attachment and is the catalytic reaction interface of microbial anaerobic respiration, which mainly affects the enrichment and growth of microorganisms, the ability of electron transfer and the resistance of electrode (Harshiny *et al.*, 2017; Hindatu *et al.*, 2017; Paul *et al.*, 2018; Wang *et al.*, 2018; Zhong *et al.*, 2018). In general, the modified anode will be an effective way to improve the electro-chemical performance and power output of the MSMFCs (Song *et al.*, 2015; Bi *et al.*, 2018).

Researchers have found that nitrogen is beneficial to

\* Corresponding authors. E-mail: ffybb@ouc.edu.cn

the electrochemical performance of the microbial fuel cells (MFCs), ascribing that nitrogen can directly affect the metabolism of microorganisms and the transfer of electrons, changing the bioelectrochemical performance of the MFCs (Asghar *et al.*, 2017; Liang *et al.*, 2019). Meanwhile, the increase of N/C content can reduce the activation energy of the reaction, which assists to increase electron transfer kinetic activity and further accelerate the electron transfer (Cheng *et al.*, 2007; Wang *et al.*, 2009; Saito *et al.*, 2011). In addition, the electrical property of the bacterial cell wall composed of lipophosphate ( $-\text{PO}_4^{3-}$ ) is negative. While the nitrogen element has strong electronegativity, and there is strong adsorption effect on microorganisms, which are propitious to the enrichment of bacteria on the surface of the anode. 3-aminopropyl-triethoxysilane (KH550) is a type of low-molecular weight organosilicon compound containing two amino groups. It possesses two active functional groups, which can serve as a bridge connecting metal ions and carbon felt anodes (Wei *et al.*, 2018).

At present, the electrogenic microorganisms isolated in natural conditions mainly belong to *Proteobacteria* and *firmicutes*, a kind of facultative anaerobic bacteria, which their metabolic modes are anaerobic respiration and fermentation. Most of these electrogenic microorganisms are iron-reducing bacteria in which Fe(III) is the final electron acceptor (Fan *et al.*, 2018; Ren *et al.*, 2018). Therefore,  $\text{Fe}^{3+}/\text{Fe}^{2+}$  and other variable valence metals can act as an intermediary for extracellular electron transfer, increasing the rate of electron transfer and further increasing the kinetic activity and output power (Huang *et al.*, 2017; Liu *et al.*, 2018).

In previous studies, the traditional way to increase the nitrogen content on the surface of materials is to dope nitrogen in the carbon lattice. However, 3-aminopropyl-triethoxysilane was grafted onto the surface of carbon felt anode using chemical method, and a composite modified

anode was prepared through organic ligands (KH550) coordination  $\text{Fe}^{3+}$  in this paper. Compared with the traditional way, grafting amino groups on the surface of carbon materials is more propitious to the growth and enrichment of microorganisms. In addition, this modification method realizes directly grafting of  $\text{Fe}^{3+}$  on the surface of the anode materials by KH550, and it aims to enhance the electron transfer efficiency. Meanwhile, this research enriches the connotation of nitrogen modification and expands the novel ideas for the subsequent research on the cell anode modification. Furthermore, the method is simple and easy to implement in real sea and the modification process does not introduce environmental damage factors, and is compatible with environmental protection concepts.

## 2 Materials and Methods

### 2.1 Preparation of Modified Anode

Carbon felt chosen as the anode of the MSMFCs was ultrasonically washed by acetone and then by distilled water for 15 min respectively before use. The pretreated carbon felt was immersed in  $\text{HNO}_3$  ( $16 \text{ mol L}^{-1}$ ) and incubated at  $90^\circ\text{C}$  for 2 h. The oxidized carbon felt was immersed in 0.5% KH550 solution and refluxed at  $100^\circ\text{C}$  for 2 h. The carbon felt was then washed with distilled water to remove the residual KH550 (Cui *et al.*, 2018). KH550 modified carbon felt was placed in  $3.5 \text{ g L}^{-1}$   $\text{FeCl}_3$  solution for 5 h (Zhang *et al.*, 2015). Titanium wires ( $\Phi 1.0 \text{ mm}$ ) were fixed onto carbon felts with projected surface areas of  $18 \text{ cm}^2$  to form anodes ( $3.0 \text{ cm} \times 3.0 \text{ cm} \times 0.3 \text{ cm}$ ). Four different anodes were named respectively as follows: i) unmodified anode (blank); ii) oxidation treatment (Oxide); iii) modification with 3-aminopropyl-triethoxysilane (KH550); iv) composite modified anode (KH 550- $\text{Fe}^{3+}$ ). The preparation process is shown in Fig.1.

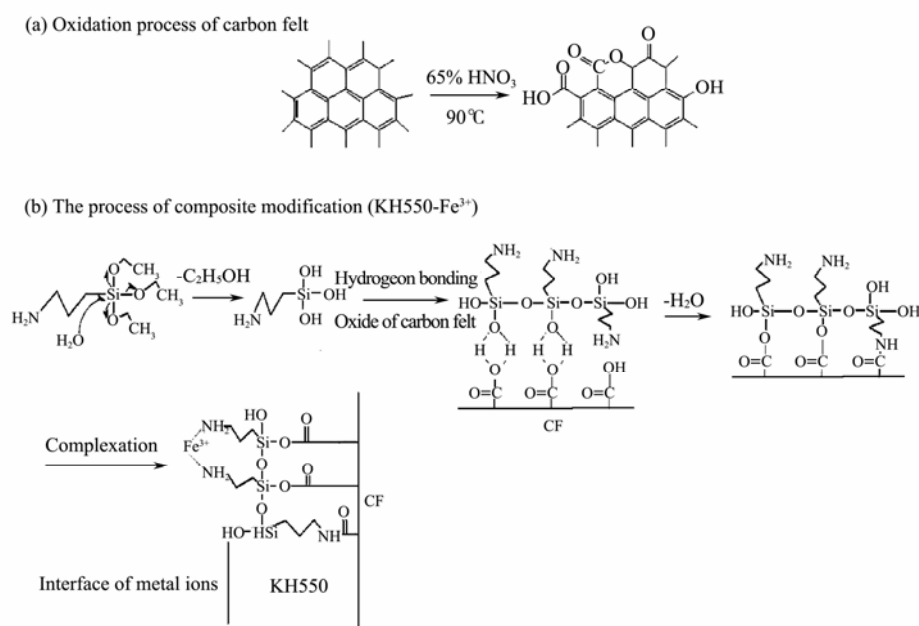


Fig.1 The preparation process of modification (CF, carbon felt).

## 2.2 The Construction of MSMFCs

Natural sea mud samples (600 g of each group) were added into a beaker with a capacity of 500 mL. The modified carbon felt anodes were embedded into the sediment and the bottom of each electrode is 2 cm away from the bottom of the beaker. Natural seawater instead of buffer solution works as electrolyte in the MSMFCs. The MSMFCs were constructed with different anodes and a shared big size cathode through a salt bridge. Moreover, their large-size cathode was composed of the same carbon brush and was completely submerged in a flume filled fully with sea water.

## 2.3 Testing and Characterization

Molecular structures on different anodes were characterized by Fourier transform infrared spectroscopy (FT-IR). Scanning electron microscope (SEM) and energy dispersive X-ray spectrometry (EDS) were utilized to examine the microscopic patterns of different electrodes (Zhang *et al.*, 2018). The attached bacteria amount was estimated by fluorescence microscopy (Fu *et al.*, 2016; Guo *et al.*, 2018). 10 g sea mud fetched on the anode surface was uniformly dispersed in 50 mL sterilized seawater, and bacteria were enriched on 0.22  $\mu\text{m}$  micro pore filter film after fine filtration. The filter film was dyed by 4',6-diamidino-2-phenylindole (DAPI) and then observed under fluorescence microscopy with a magnification 400 $\times$  to calculate the bacterial colony amount. According to the formula,  $N = Na * S / St$ ,  $Na$  – average amount in each vision,  $S$  – carbon felt area  $\text{m}^2$ ,  $St$  – whole vision area  $\text{m}^2$ .

All electrochemical analysis were conducted by CHI660E electrochemical workstation by a three-electrode system composed of a carbon felt as working electrode, an Ag/AgCl as reference electrode and a 9.0  $\text{cm}^2$  of platinum as counter electrode. Tafel plot, cyclic voltam-

metry (CV) and electrochemical impedance spectra (EIS) were measured to evaluate the electrochemical performance of anodes. Electrochemical activity of redox was characterized by the CV (within the potential window from  $-0.8\text{ V}$  to  $0.3\text{ V}$  vs. Ag/AgCl at a scan rate of  $1.0\text{ mV s}^{-1}$ ). Tafel plots were recorded at a scan rate of  $1.0\text{ mV s}^{-1}$  from  $-200\text{ mV}$  to  $200\text{ mV}$  around open circuit potential (OCP). The EIS was collected at OCP using 5.0 mV perturbation in a frequency range of 20 kHz to 10 mHz. The maximum power density and polarization curves of the MSMFC were conducted by adjusting the external resistance from  $90000\ \Omega$  to  $100\ \Omega$  for evaluating the performance of different MSMFCs.

## 3 Results and Discussion

### 3.1 Surface Molecules and Structure Characteristics of Different Anodes

As shown in Fig.2, the functional groups are described as follows: The peak in the region of  $3445\text{ cm}^{-1}$  shows the existence of O-H for oxidized sample. The appearance of the bands in the region from  $3480\text{ cm}^{-1}$  to  $3550\text{ cm}^{-1}$  means the existence of stretching vibration peak of N-H in KH550 modified anode. Meanwhile, the characteristic bands locating in  $1687\text{ cm}^{-1}$ ,  $1530\text{ cm}^{-1}$  and  $1358\text{ cm}^{-1}$  indicate the existence of amide I, II and III bands respectively. Furthermore, the characteristic peak of CO-OR appears at  $1722\text{ cm}^{-1}$  and C-O-Si vibration peak at  $1180\text{ cm}^{-1}$  respectively (Cui *et al.*, 2018) and their intensities of stretching vibration peaks of  $-\text{CH}_2-$  and  $-\text{CH}_3$  at  $2830\text{ cm}^{-1}$  and  $2960\text{ cm}^{-1}$  respectively become stronger, which is ascribed to the introduction of KH550. Moreover, the N-H stretching vibration peaks of the composite modified anode move toward small wave number and their strength decreases (Fig.2b) (Hu *et al.*, 2015; Wang *et al.*, 2019). The reason may be that its complexation between  $\text{Fe}^{3+}$  and  $-\text{NH}_2$  weakens the strength of the N-H bond.

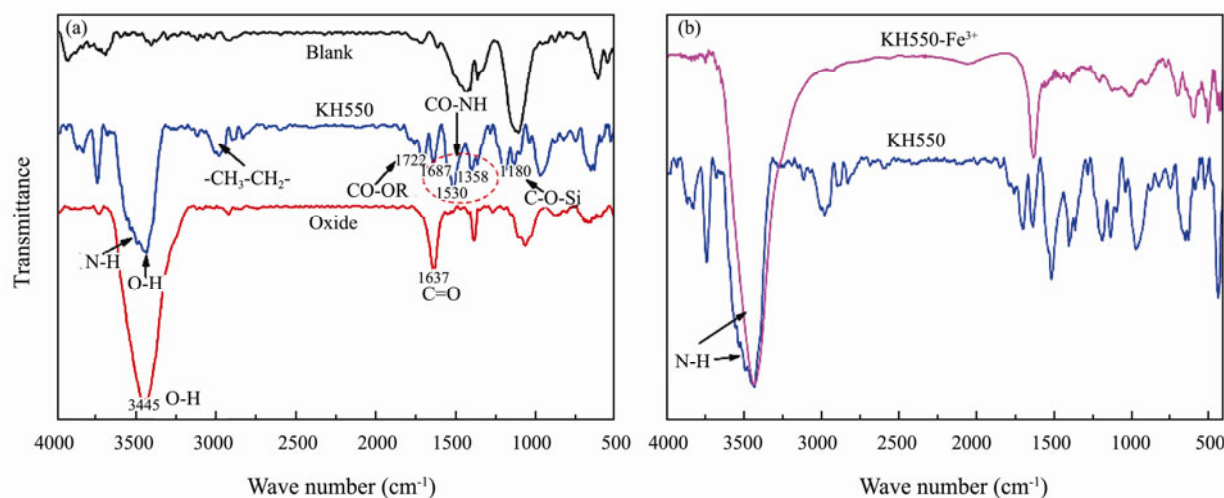


Fig.2 FT-IR patterns of different anodes. (a), Modified and unmodified anode; (b), Comparison between KH550 and KH550- $\text{Fe}^{3+}$ .

SEM indicates that the grooves on the unmodified carbon felt surface are narrow and has more impurities (Fig.

3a). After oxidation treatment, its surface is slightly etched, and the grooves become wide and deep (Fig.3b). A

uniform film has formed on the surface of composite modified carbon felt (Fig.3c). By EDS analysis (Fig.3d), its surface contains Si, N, Fe and other elements. Combined with infrared analysis, amide I, II and III bands

exist on the surface of carbon felt and the intensity of N-H stretching vibration peaks decreases, indicating that KH550-Fe<sup>3+</sup> composite modified anode is successfully prepared by this method.

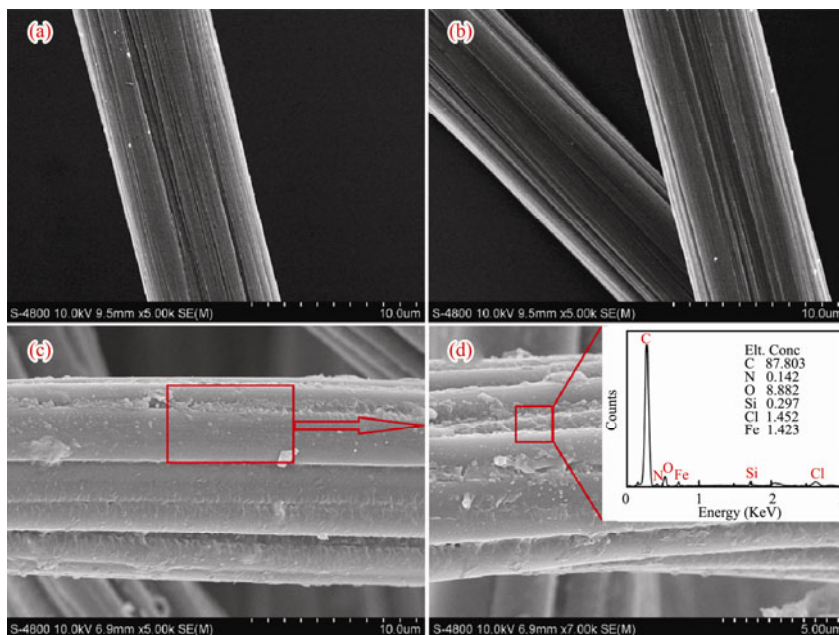


Fig.3 Surface morphologies of different anodes. (a), Blank anode; (b), Oxide; (c), KH550-Fe<sup>3+</sup> modified anode; (d), EDS analysis of KH550-Fe<sup>3+</sup> modified anode.

### 3.2 Microbial Analysis on Anodic Surface

The quantitative comparison of biomass on different anode surfaces is shown in Fig.4 and Table 1. According to the formula  $N = Na \times S / St$  (Fu *et al.*, 2016), where  $Na$  is the average bacteria amount in a vision field;  $S$  the

surface area of carbon felt;  $St$  the counting vision area, the amount of microorganisms on composite modified anode ( $3.4 \times 10^{11} \text{ m}^{-2}$ ) and KH550 modified anode ( $3.3 \times 10^{11} \text{ m}^{-2}$ ) are 4.8 times and 4.6 times higher than that of unmodified anode, respectively. That demonstrates that KH550 promotes the growth and attachment of bacteria on anode.

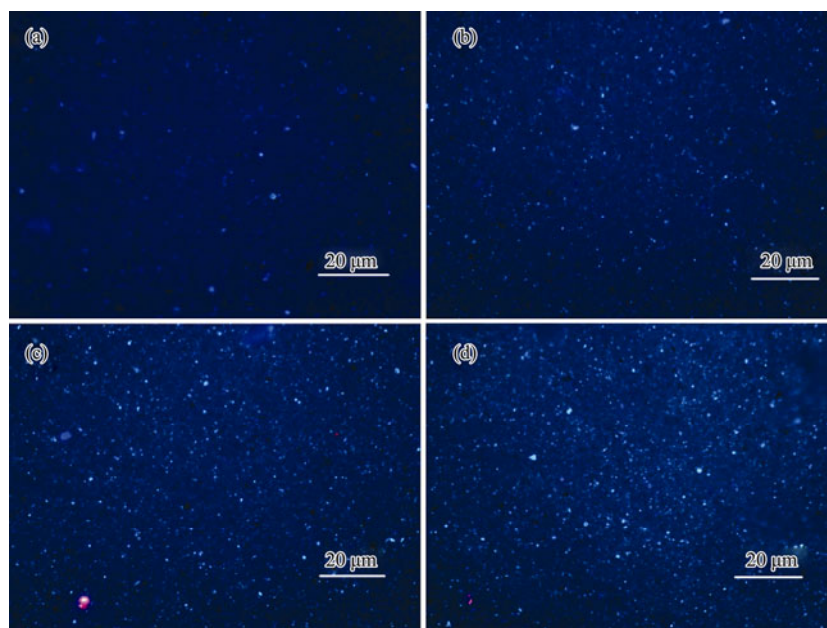


Fig.4 Microbial fluorescence photos on different anodic surfaces. (a), Blank anode; (b), Oxide; (c), KH550 modified anode; (d), KH550-Fe<sup>3+</sup> modified anode.

Table 1 Microbial quantities on different anodic surfaces

Anodes	Blank	Oxide	KH550	KH550-Fe <sup>3+</sup>
Average (10 <sup>10</sup> m <sup>-2</sup> )	7.1	18.0	33.0	34.0
Ratio	1	2.5	4.6	4.8

### 3.3 Electrochemical Measurement and Analysis

#### 3.3.1 Cyclic voltammetry test

CV curves and their capacitive performances of different electrodes are revealed in Fig.5 and Table 2. The different anodes show obvious oxidation peaks approaching to -0.00922 V, -0.0546 V and -0.0304 V respectively, which are attributed to the redox with consumption of organic compounds *via* the catalyzation of bacteria. The maximum oxidation peak current density of KH550-Fe<sup>3+</sup> is 1.528 A m<sup>-2</sup>, which is 5.3 times higher than that of blank anode (0.288 A m<sup>-2</sup>). It indicates that the introduction of an amino-group and a ferric ion is effective to increase the electrochemical activity of microorganisms in the anode biofilm. According to the formula (Dong et al., 2015)

$$C = \frac{1}{s \cdot A \cdot \Delta V} \int_{V_0}^{V_0 + \Delta V} i dV,$$

C is specific capacity (F cm<sup>-2</sup>), s is sweep velocity (Vs<sup>-1</sup>), A is anodic area (cm<sup>2</sup>), ΔV is potential window (V), I is cur-

rent (A), specific capacitance of different anodes can be calculated respectively. The specific capacitances of composite modified anode (887.8 F m<sup>-2</sup>) and KH550 modified anode (482.8 F m<sup>-2</sup>) are 3.7 times and 2.0 times of blank anode (23.74 F m<sup>-2</sup>) respectively. Among them, the KH 550-Fe<sup>3+</sup> composite anode has the largest capacitance, which indicates that the chelation of Fe<sup>3+</sup> with KH550 effectively improves anode ability to capture electrons.

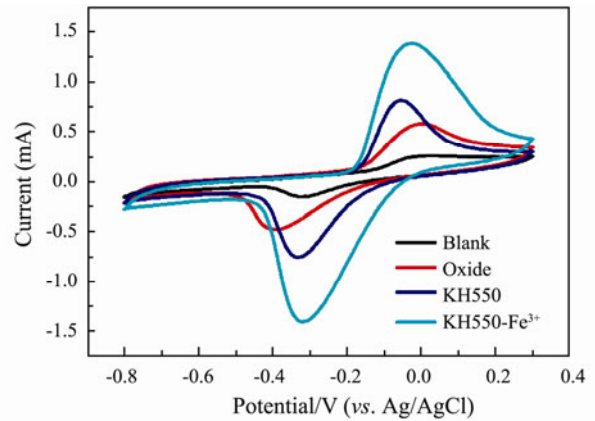


Fig.5 Cyclic voltammetry curves of different anodes: Blank anode (line black); oxide (line red); KH550 modified anode (line blue); KH550-Fe<sup>3+</sup> modified anode (line dark cyan).

Table 2 Parameters of anodic CV curves

Anode	S (V mA)	C (F m <sup>-2</sup> )	E (V, vs. Ag/AgCl)	i (A m <sup>-2</sup> )
Blank	0.235	237.4	-0.00391	0.288
Oxide	0.4049	408.9	-0.0092	0.626
KH550	0.478	482.8	-0.0545	0.887
KH550-Fe <sup>3+</sup>	0.879	887.8	-0.0304	1.528

#### 3.3.2 Tafel curves

The exchange current density exhibits the instantaneous kinetic activity of the anode. If it becomes higher, the activation energy of the reaction will be lower, its redox reaction is faster and its time required for the electrode to reach equilibrium will be shorter (Guo et al., 2018). The Tafel curves of different anodes are shown in Fig.6. Ac-

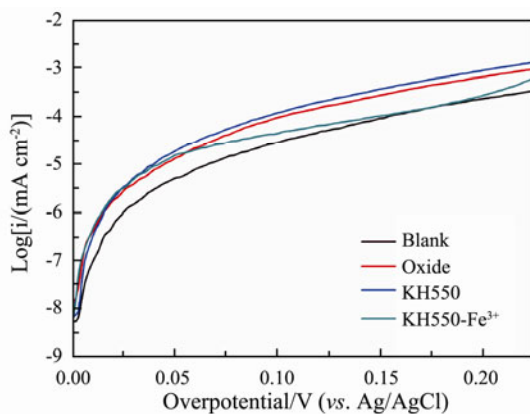


Fig.6 Tafel curves of different anodes: Blank anode (line black); oxide (line red); KH550 modified anode (line blue); KH550-Fe<sup>3+</sup> modified anode (line dark cyan).

cording to the formula  $\eta = a + b \log|i|$ , linear fitting is performed using extrapolation (Table 3). The exchange current densities of the KH550 and KH550-Fe<sup>3+</sup> anode are 3.4 times and 5.8 times higher than that of the blank anode, indicating that both amino modification and composite modification have significantly improved kinetic activity and anti-polarization ability.

Table 3 Parameters of anodic Tafel curves

Anode	OCP/(V, vs. Ag/AgCl)	i <sub>0</sub> /(×10 <sup>-7</sup> mA cm <sup>-2</sup> )	KA
Blank	-0.428	9.10	1.0
Oxide	-0.382	17.8	1.9
KH550	-0.346	31.0	3.4
KH550-Fe <sup>3+</sup>	-0.336	52.5	5.8

#### 3.3.3 Polarization test

The polarization curves of the different anodes are presented in Fig.7, and their anodic anti-polarization ability is KH550-Fe<sup>3+</sup> > KH550 > Oxide > Blank. The polarization curves are analyzed according to the low current region, the middle and the high current regions respectively. The slope of each section is obtained by linear fitting as shown in Table 4. The larger the slope value, the weaker the anti-polarization ability of the anode. In the

middle current region, the controlling factors for this region are the properties of anode surface and the amounts of enriched microorganisms. The amino-group improves the enrichment of microorganisms on the surface of the anode to ensure the output of electrons and enhances the anti-polarization ability. Meanwhile, a few amino-groups act as ligand to coordinate  $\text{Fe}^{3+}$  forming large steric hindrance, which would hinder mass transfer from mud to anode itself, so the anti-polarization ability of KH550 is stronger than that of KH550- $\text{Fe}^{3+}$  in this region. In its high current region, the anti-polarization ability of the composite anode is the best among them, because the valence transformation between  $\text{Fe}^{3+}$  and  $\text{Fe}^{2+}$  acting as intermediary increases the electron transfer rate to the anode surface. This anti-polarization is very important performance for the MSMFCs as a power source, especially when it drives the marine instrument to work in high current.

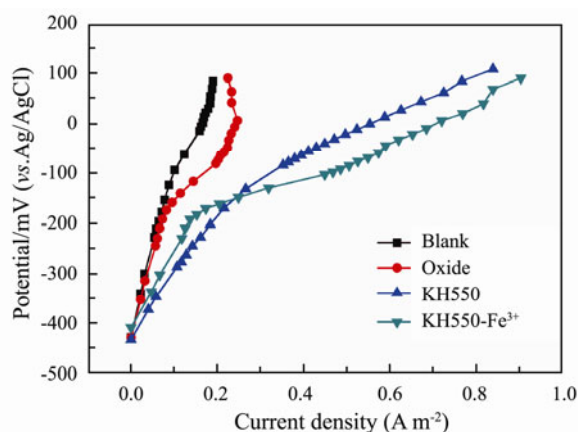


Fig. 7 Polarization curves of different anodes. Blank anode (line black); oxide (line red); KH550 modified anode (line blue); KH550- $\text{Fe}^{3+}$  modified anode (line dark cyan).

Table 4 Slope values of different polarizations in different regions

Current (mA)	Blank	Oxide	KH550	KH550- $\text{Fe}^{3+}$
0–0.08	3753	3167	1383	1530
0.08–0.18	1890	1400	1092	1292
0.18–0.9	6122	2362	421	379

### 3.3.4 Electrochemical impedance spectroscopy

After the continuous and stable discharge, the different anodic electrochemical impedances are conducted, and their results are fitted with Zview software to obtain the fitting curves, the equivalent circuits and impedances fitting parameters are shown in Fig. 8 and Table 5. Among them,  $CPE-1$ ,  $CPE-2$  and  $R_f$  are the electric double layer capacitance of the anode, biofilm capacitance and the biofilm resistance, respectively.

The results illustrate that the charge transfer resistances ( $R_{ct}$ ) of amino-group modified and its composite modified anode are both lower than that of unmodified anode, and KH550- $\text{Fe}^{3+}$  is less than that of KH550. The reason is that nitrogen element directly affects the metabolism of mi-

croorganisms and it is conducive to the adsorption of negatively charged microorganisms. In addition, the increase of N/C content can reduce the activation energy of the reaction and accelerate the electron transfer, which is beneficial to enhance electron transfer kinetic activity. In general, doping N atoms in carbon lattice is the dominating method of increasing nitrogen content (Ratso et al., 2017). However, this method has some drawbacks. Only a small portion of the introduced nitrogen atoms are exposed at the interface of electrodes/sea water. In this study, we introduce free amino groups by chemical grafting, which will cause much larger contact area between amino group and microorganism, resulting in the enrichment of great amount of microorganisms on the anode, as seen in the Fig. 4.

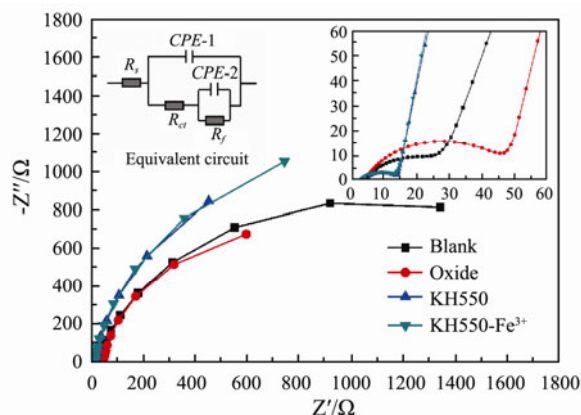


Fig. 8 The electrochemical impedance fitting curves and the equivalent circuit diagram of different anodes. Blank anode (line black); oxide (line red); KH550 modified anode (line blue); KH550- $\text{Fe}^{3+}$  modified anode (line dark cyan).

Table 5 The fitting values of the EIS

Anodes	Blank	Oxide	KH550	KH550- $\text{Fe}^{3+}$
$R_s$ ( $\Omega$ )	4.477	4.141	3.863	2.538
$CPE-1-T$ ( $\times 10^{-4} \Omega^{-1} \text{cm}^{-2} \text{s}^{-n}$ )	4.747	3.540	5.330	8.194
$CPE-1-P \times 10^{-2}$	73.16	75.68	68.05	62.61
$R_{ct}$ ( $\Omega$ )	24.04	44.99	10.5	10.11
$CPE-2-T$ ( $\times 10^{-3} \Omega^{-1} \text{cm}^{-2} \text{s}^{-n}$ )	3.788	11.65	11.88	8.362
$CPE-2-P \times 10^{-2}$	86.25	92.55	91.64	92.51
$R_f$ ( $\Omega$ )	2100	1605	2765	2707

Moreover, the valence transformation of iron ion also accelerates the electron transfer efficiency and reduces the charge transfer resistance, which is consistent with the analysis results in the polarization curves (Fig. 7). The electric double layer capacitance of composite modified anode is higher than that of blank anode, which is corroborated by the results of cyclic voltammetry (Fig. 5). Its biofilm resistance (2707  $\Omega$ ) is 1.3 times higher than that of blank anode (2100.3  $\Omega$ ) and the biofilm capacitance also increases by 2.2 times. This illustrates that composite modification improves bacteria adhesion on its anode surface due to the existence of amino group. The chelation of  $\text{Fe}^{3+}$  provides an intermediary for electron transfer.

Composite modification could cause not only the increase in higher amount of bacteria, but also the improvement of efficiency in electron transfer, and further synergistically improves the exchange current density, which is consistent with the Tafel test results (Fig.6).

### 3.4 Battery Performance

#### 3.4.1 Power density

As shown in Fig.9, the output power of the composite modification MSMFC ( $203.8 \text{ mW m}^{-2}$ ) is 4.5 times higher than that of the unmodified MSMFC ( $45.07 \text{ mW m}^{-2}$ ), and its output current density also increases by 4.4 times. That might be ascribed to the fact that amino modification increases the amount of microbial attachment on the anode, and  $\text{Fe}^{3+}$  acts as charge transfer medium to enhance the electron transfer efficiency, finally improving the performance of power. However, Ci *et al.* (2012) have studied nitrogen-doped carbon and indicated that the power of MFC modified by nitrogen-doped carbon nanotubes enhance 1.6 times compared with unmodified MFC. Therefore, compared with the nitrogen doping in carbon lattice, grafting amino groups on the surface of carbon materials is more propitious to the improvement of MSMFCs output.

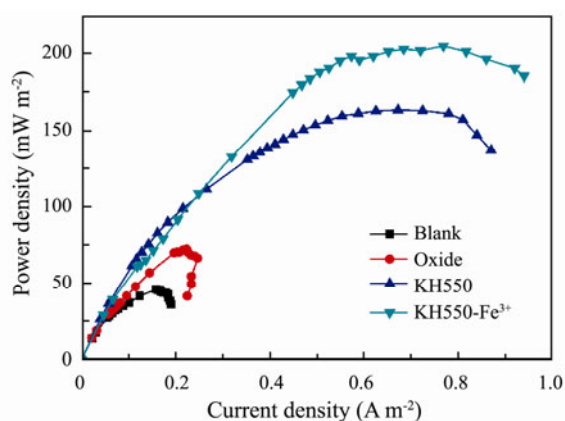


Fig.9 The power density curves of MSMFCs with different anodes: Blank anode (line black); oxide (line red); KH550 modified anode (line blue); KH550- $\text{Fe}^{3+}$  modified anode (line dark cyan).

#### 3.4.2 Long-term discharge test

In Fig.10, the voltages of Oxide, KH550, KH550- $\text{Fe}^{3+}$  batteries keep ready state at 554 mV, 733 mV, 795 mV respectively, and blank battery at 386 mV, indicating that KH550 and KH550- $\text{Fe}^{3+}$  modification significantly improves the battery production performance. In addition, comparing the voltage difference between KH550 and KH550- $\text{Fe}^{3+}$  batteries, it also confirms that the amino group plays a greater role than  $\text{Fe}^{3+}$  in electricity production.

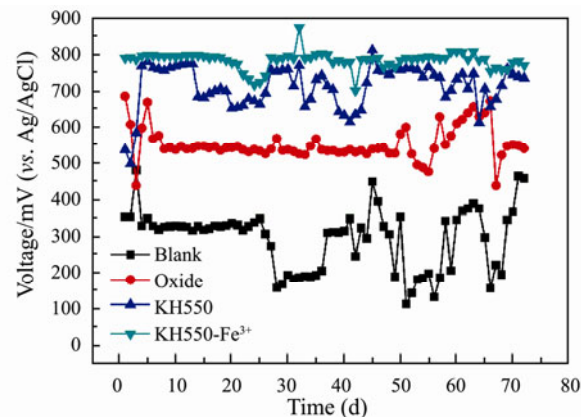


Fig.10 Long-term discharge curves of the MSMFCs with different anodes: Blank anode (line black); oxide (line red); KH550 modified anode (line blue); KH550- $\text{Fe}^{3+}$  modified anode (line dark cyan).

### 3.5 Mechanism Analysis

A novel mechanism of KH550- $\text{Fe}^{3+}$  composite modified anode is shown in Fig.11 for explanation of its anodic excellent electrochemical and battery performance.

On the one hand, amino group modifies carbon felt to increase its N/C ratio, which directly affects the metabolism of microorganisms and properties of anode surface (Ci *et al.*, 2012). Compared with the nitrogen doping in carbon lattice, grafting amino groups on the surface of carbon materials is more propitious to the growth and enrichment of microorganisms owing to the larger contact area between amino group and microorganism.

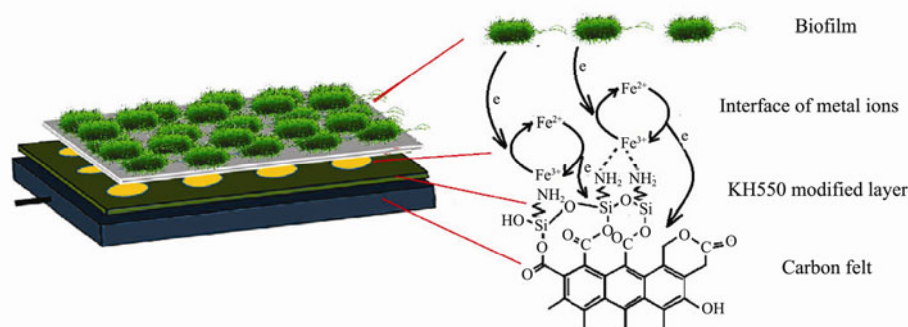


Fig.11 The synergistic mechanism of KH550- $\text{Fe}^{3+}$  composite modified anode.

On the other hand, this modification method realizes directly coordination of  $\text{Fe}^{3+}$  by amino group and  $\text{Fe}^{3+}/\text{Fe}^{2+}$  valence transformation acts as an electron transfer

shuttle to enhance the kinetic efficiency of electron transfer, and further improves the battery performance (Hu *et al.*, 2015).

In addition, this research enriches the connotation of nitrogen modification and expands the novel ideas for the subsequent research on the modification of battery in real sea. Furthermore, the method is simple and easy to implement in large scale and the modification process is benign to environment.

## 4 Conclusions

3-aminopropyltriethoxysilane complexation with iron ion was successfully utilized to modify the anode in the MSMFCs and significantly improves its electrochemical performance. The composite modified MSMFC generates the higher power densities than the blank ( $203.8 \text{ mW m}^{-2}$  versus  $45.07 \text{ mW m}^{-2}$ ), and its current also increases by 4.4 times. Compared with the nitrogen doping in carbon electrode, this research enriches the connotation of nitrogen modification of carbon electrode material and expands the novel ideas for the subsequent research on the modification of cell anode in a large scale fabrication. Finally, the research inspires a new idea that the modified anode by amino group can coordinate the natural  $\text{Fe}^{3+}$  ions in ocean for its long term power production.

## Acknowledgement

This work was supported by the National Natural Science Foundation of China (No. 22075262). This work is in compliance with ethical standards. The authors declare that they have no conflict of interest for this work.

## References

- Asghar, A., Raman, A. A. A., Daud, W. M. A. W., Ahmad, M., and Zain, S. U. B. M., 2017. Effect of nitrogen doping on graphite cathode for hydrogen peroxide production and power generation in MFC. *Journal of the Taiwan Institute of Chemical Engineers*, **76**: 89-100, DOI: 10.1016/j.jtice.2017.04.016.
- Bi, L. L., Ci, S. Q., Cai, P. W., Li, H., and Wen, Z. H., 2018. One-step pyrolysis route to three dimensional nitrogen-doped porous carbon as anode materials for microbial fuel cells. *Applied Surface Science*, **427**: 10-16, DOI: 10.1016/j.apsusc.2017.08.030.
- Chen, W., Liu, Z. H., Su, G., Fu, Y. B., Zai, X. R., Zhou, C. Y., and Wang, J., 2017. Composite-modified anode by  $\text{MnO}_2$ /polypyrrole in marine benthic microbial fuel cells and its electrochemical performance. *International Journal of Energy Research*, **41** (6): 845-853, DOI: 10.1002/er.3674.
- Cheng, S., and Logan, B. E., 2007. Ammonia treatment of carbon cloth anodes to enhance power generation of microbial fuel cells. *Electrochemistry Communications*, **9** (3): 492-496, DOI: 10.1016/j.elecom.2006.10.023.
- Ci, S. Q., Wen, Z. H., Chen, J. H., and He, Z., 2012. Decorating anode with bamboo-like nitrogen-doped carbon nanotubes for microbial fuel cells. *Electrochemistry Communications*, **14** (1): 71-74, DOI: 10.1016/j.elecom.2011.11.006.
- Cui, H. Z., Jin, Z. Y., Zheng, D. P., Tang, W. C., Li, Y., Yun, Y. C., Lo, T. Y., and Xing, F., 2018. Effect of carbon fibers grafted with carbon nanotubes on mechanical properties of cement-based composites. *Construction and Building Materials*, **181**: 713-720, DOI: 10.1016/j.conbuildmat.2018.06.049.
- Dong, L. B., Xu, C. J., Yang, Q., Fang, J., Li, Y., and Kang, F. Y., 2015. High-performance compressible supercapacitors based on functionally synergic multiscale carbon composite textiles. *Journal of Materials Chemistry A*, **3** (8): 4729-4737, DOI: 10.1039/C4TA06494A.
- Ewing, T., Ha, P. T., and Beyenal, H., 2017. Evaluation of long-term performance of sediment microbial fuel cells and the role of natural resources. *Applied Energy*, **192**: 490-497, DOI: 10.1016/j.apenergy.2016.08.177.
- Fan, Y. Y., Li, B. B., Yang, Z. C., Cheng, Y. Y., Liu, D. F., and Yu, H. Q., 2018. Abundance and diversity of iron reducing bacteria communities in the sediments of a heavily polluted freshwater lake. *Applied Microbiology and Biotechnology*, **102** (24): 10791-10801, DOI: 10.1007/s00253-018-9443-1.
- Fu, Y. B., Liu, Z. H., Su, G., Zai, X. R., Ying, M., and Yu, J., 2016. Modified carbon anode by MWCNTs/PANI used in marine sediment microbial fuel cell and its electrochemical performance. *Fuel Cells*, **16** (3): 377-383, DOI: 10.1002/fuce.201500103.
- Ghoreishi, K. B., Ghasemi, M., Rahimnejad, M., Yarmo, M. A., Daud, W. R. W., Asim, N., and Ismail, M., 2014. Development and application of vanadium oxide/polyaniline composite as a novel cathode catalyst in microbial fuel cell. *International Journal of Energy Research*, **38** (1): 70-77, DOI: 10.1002/er.3082.
- Guo, M., Zai, X. R., Li, T., Zhang, H. J., Zhao, Y. G., Zhao, M. G., Liu, S., Ji, H. W., and Fu, Y. B., 2018. Effect of amino acid addition in marine sediment on electrochemical performance in microbial fuel cells. *Fuel Cells*, **18** (4): 518-525, DOI: 10.1002/fuce.201800021.
- Harshiny, M., Samsudeen, N., Kameswara, R. J., and Matheswaran, M., 2017. Biosynthesized  $\text{FeO}$  nanoparticles coated carbon anode for improving the performance of microbial fuel cell. *International Journal of Hydrogen Energy*, **42**: 26488-26495, DOI: 10.1016/j.ijhydene.2017.07.084.
- Hindatu, Y., Annuar, M. S. M., and Gumel, A. M., 2017. Mini-review: Anode modification for improved performance of microbial fuel cell. *Renewable and Sustainable Energy Reviews*, **73**: 236-248, DOI: 10.1016/j.rser.2017.01.138.
- Hu, Q. L., Chen, N., Feng, C. P., and Hu, W. W., 2015. Nitrate adsorption from aqueous solution using granular chitosan- $\text{Fe}^{3+}$  complex. *Applied Surface Science*, **347**: 1-9, DOI: 10.1016/j.apsusc.2015.04.049.
- Huang, W. T., Chen, J. F., Hu, Y. Y., Chen, J., Sun, J., and Zhang, L. H., 2017. Enhanced simultaneous decolorization of azo dye and electricity generation in microbial fuel cell (MFC) with redox mediator modified anode. *International Journal of Hydrogen Energy*, **42** (4): 2349-2359, DOI: 10.1016/j.ijhydene.2016.09.216.
- Liang, B. L., Li, K. X., Liu, Y., and Kang, X. W., 2019. Nitrogen and phosphorus dual-doped carbon derived from chitosan: An excellent cathode catalyst in microbial fuel cell. *Chemical Engineering Journal*, **358**: 1002-1011, DOI: 10.1016/j.cej.2018.09.217.
- Liu, Q., Yang, Y., Mei, X. X., Liu, B. F., Chen, C., and Xing, D. F., 2018. Response of the microbial community structure of



- biofilms to ferric iron in microbial fuel cells. *Science of the Total Environment*, **631**: 695-701, DOI: 10.1016/j.scitotenv.2018.03.008.
- Paul, D., Noori, M. T., Rajesh, P. P., Ghangrekar, M. M., and Mitra, A., 2018. Modification of carbon felt anode with graphene oxide-zeolite composite for enhancing the performance of microbial fuel cell. *Sustainable Energy Technologies and Assessments*, **26**: 77-82, DOI: 10.1016/j.seta.2017.10.001.
- Ratso, S., Kruusenberg, I., Käärik, M., Kook, M., Saar, R., Pärs, M., Leis, J., and Tammeveski, K., 2017. Highly efficient nitrogen-doped carbide-derived carbon materials for oxygen reduction reaction in alkaline media. *Carbon*, **113**: 159-169, DOI: 10.1016/j.carbon.2016.11.037.
- Ren, G. P., Sun, Y., Lu, A. H., Li, Y., and Ding, H. R., 2018. Boosting electricity generation and Cr(VI) reduction based on a novel silicon solar cell coupled double-anode (photoanode/bioanode) microbial fuel cell. *Journal of Power Sources*, **408**: 46-50, DOI: 10.1016/j.jpowsour.2018.10.081.
- Saito, T., Mehanna, M., Wang, X., Cusick, R. D., Feng, Y., Hickner, M. A., and Logan, B. E., 2011. Effect of nitrogen addition on the performance of microbial fuel cell anodes. *Bioresource Technology*, **102** (1): 395-398, DOI: 10.1016/j.biortech.2010.05.063.
- Song, Y., Kim, D., Woo, J., Subha, B., Jang, S., and Sivakumar, S., 2015. Effect of surface modification of anode with surfactant on the performance of microbial fuel cell. *International Journal of Energy Research*, **39** (6): 860-868, DOI: 10.1002/er.3284.
- Wang, S. Q., Zhao, N. Q., Shi, C. S., Liu, E. Z., He, C. N., He, F., and Ma, L. Y., 2018. *In-situ* grown CNTs modified SiO<sub>2</sub>/C composites as anode with improved cycling stability and rate capability for lithium storage. *Applied Surface Science*, **433**: 428-436, DOI: 10.1016/j.apsusc.2017.10.057.
- Wang, X., Cheng, S. A., Feng, Y. J., Merrill, M. D., Saito, T., and Logan, B. E., 2009. Use of carbon mesh anodes and the effect of different pretreatment methods on power production in microbial fuel cells. *Environmental Science & Technology*, **43** (17): 6870-6874, DOI: 10.1021/es900997w.
- Wang, Y. X., de Souza Borges Ferreira, R., Wang, R. X., Qiu, G., Li, G. D., Qin, Y., Ye, P. D., Sabbaghi, A., and Wu, W. Z., 2019. Data-driven and probabilistic learning of the process-structure-property relationship in solution-grown tellurene for optimized nanomanufacturing of high-performance nano-electronics. *Nano Energy*, **57**: 480-491, DOI: 10.1016/j.nanoen.2018.12.065.
- Wei, Q., and Wang, W. H., 2018. Properties of phenol formaldehyde resin modified with silane coupling agent (KH550). *International Journal of Adhesion and Adhesives*, **84**: 166-172, DOI: 10.1016/j.ijadhadh.2018.03.006.
- Zhang, H. S., Fu, Y. B., Zhou, C. Y., Liu, S., Zhao, M. G., Chen, T. L., and Zai, X. R., 2018. A novel anode modified by 1,5-dihydroxyanthraquinone/multiwalled carbon nanotubes composite in marine sediment microbial fuel cell and its electrochemical performance. *International Journal of Energy Research*, **42** (7): 2574-2582, DOI: 10.1002/er.4034.
- Zhang, J., Chen, N., Tang, Z., Yu, Y., Hu, Q., and Feng, C., 2015. A study of the mechanism of fluoride adsorption from aqueous solutions onto Fe-impregnated chitosan. *Physical Chemistry Chemical Physics*, **17** (18): 12041-12050, DOI: 10.1039/c5cp00817d.
- Zhao, Q., Ji, M., Li, R. Y., and Ren, Z. J., 2017. Long-term performance of sediment microbial fuel cells with multiple anodes. *Bioresource Technology*, **237**: 178-185, DOI: 10.1016/j.biortech.2017.03.002.
- Zhong, D., Liao, X., Liu, Y., Zhong, N., and Xu, Y., 2018. Quick start-up and performance of microbial fuel cell enhanced with a polydiallyldimethylammonium chloride modified carbon felt anode. *Biosensors & Bioelectronics*, **119**: 70-78, DOI: 10.1016/j.bios.2018.07.069.
- Zhou, C. Y., Fu, Y. B., Zhang, H. S., Chen, W., Liu, Z., Liu, Z. H., Ying, M., and Zai, X. R., 2018. Structure design and performance comparison of large-scale marine sediment microbial fuel cells in lab and real sea as power source to drive monitoring instruments for long-term work. *Ionics*, **24** (3): 797-805, DOI: 10.1007/s11581-017-2251-2.

(Edited by Ji Dechun)